High-Throughput Synthesis and Screening of a Library of Random and Gradient Copoly(2-oxazoline)s

Richard Hoogenboom, Martin W. M. Fijten, Sanne Wijnans, Antje M. J. van den Berg, Hanneke M. L. Thijs, and Ulrich S. Schubert*

Laboratory of Macromolecular Chemistry and Nanoscience, Eindhoven University of Technology (TU/e) and Dutch Polymer Institute (DPI), Den Dolech 2, 5600 MB, Eindhoven, The Netherlands

Received July 8, 2005

Introduction. The living cationic ring opening polymerization (CROP; see Scheme 1) of 2-oxazolines was discovered in 1966.[1−3] After this discovery, the resulting biocompatible poly(2-oxazoline)s have been used for a wide variety of applications.[4−6] Moreover, amphiphilic structures are easily accessible by the sequential polymerization of a hydrophilic monomer (e.g., 2-methyl- or 2-ethyl-2-oxazoline) and a hydrophobic monomer (e.g., 2-nonyl- or 2-phenyl-2-oxazoline). Unlike block copoly(2-oxazoline)s, random copoly(2-oxazoline)s have not been extensively investigated so far. The possibility of copolymerizing different 2-oxazolines has been demonstrated by several groups;[7−9] however, reactivity ratios have only been determined for copolymerizations involving 2-phenyl-2-oxazoline (PhOx).[10] Due to the low reactivity of PhOx, the copolymerizations resulted in blocky structures instead of random or gradient copolymers. Moreover, the properties of copoly(2-oxazoline)s have not been studied in detail.

Inspired by this lack of knowledge in the literature, we decided to investigate the synthesis and properties of a library of random copolymers from 2-methyl-2-oxazoline (MeOx), 2-ethyl-2-oxazoline (EtOx), and 2-nonyl-2-oxazoline (NonOx). Such systematical copolymerization studies and corresponding structure−property investigations are reported for the first time. In polymer science, this report is the first example of a high-throughput approach in which kinetic details, library synthesis, and property screening were investigated simultaneously, providing both fundamental and application-directed insights.

Results and Discussion. The currently described work was preceded by detailed (automated parallel) kinetic investigation of the homopolymerizations of four monomers (MeOx, EtOx, NonOx, and PhOx) with four initiators at four molecular weights and two temperatures.[11] The optimal conditions from this kinetic screening (polymerization with benzyl bromide as initiator at 100 °C in *N*,*N*-dimethylacetamide) were applied to synthesize copolymers from combinations of MeOx, EtOx, and NonOx utilizing a Chemspeed ASW2000 synthesis robot.[12] For each combination, nine copolymers were synthesized with 0−100 mol % (steps of 12.5 mol %) of the second monomer, resulting in 27 parallel polymerizations. For each of the copolymerizations, the monomer conversion in time was investigated by automated sampling from the polymerization mixtures for GC analysis.[13] The measured monomer-to-solvent ratios of the polymerization mixtures before heating (Figure 1) clearly demonstrate the gradual change in monomer composition for the different copolymerization series: With increasing mole fraction of the second monomer, the ratio of the second monomer to solvent increases linearly, and the ratio of the first monomer to solvent decreases linearly. Figure 2 (top row) depicts the resulting kinetic plots in time for the 50 mol % copolymerizations. Similar kinetic plots were obtained for all other copolymerizations (only one of the polymerizations failed during the library synthesis cq. kinetic screening). The linearity of the first-order kinetic plots ($\ln\{[M]0/[M]_t\}$) confirmed a constant concentration of living polymer chains as expected for a living polymerization. Moreover, monomodal GPC traces with narrow molecular weight distributions (PDI < 1.3) were obtained for the endsamples, which is indicative of a living polymerization mechanism, as well.

Scheme 1. Schematic Representation of the CROP of 2-Oxazolines Initiated with Benzyl Bromide

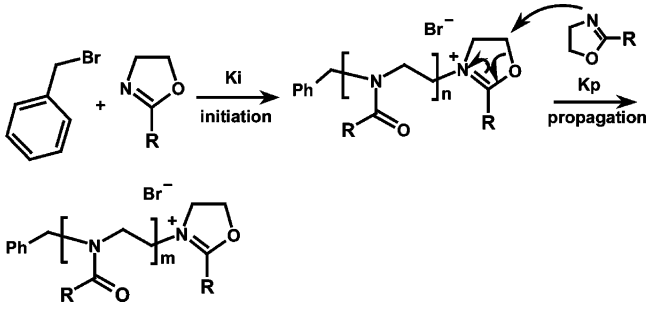

The kinetic plots revealed a slightly faster consumption (higher reactivity) of MeOx, as compared to EtOx and NonOx. To further elucidate the copolymer compositions, the reactivity ratios ($r_1 = k_{11}/k_{12}$ and $r_2 = k_{22}/k_{21}$)[14] were determined from the relation between the fraction of monomer A in the monomer feed (f_1) and the incorporated fraction of monomer A in the polymer (F_1) at both ∼20% and ∼60% monomer conversion (Figure 3.15, bottom row). For living polymerizations, the reactivity ratios should be calculated at higher monomer conversions (20% or higher) since different reactivities during the initiation process are commonly observed.[15,16] Also for the polymerization of 2-oxazolines, it is well-known that the polymerization rate during initiation can be different from the final polymerization rate.[17] In the first instance, the reactivity ratios were determined using the classical Mayo−Lewis terminal model (MLTM) utilizing nonlinear least-squares fitting of the data in Figure 2, bottom.[18] However, the applied MLMT method is strictly only valid for 0% monomer conversion, and therefore, reliable reactivity ratios can only be determined from extrapolation of the data obtained at low monomer conversions up to ∼10%. To accurately determine the

* Phone: +31 40 247 5303. Fax: +31 40 247 4186. E-mail: u.s.schubert@tue.nl.

10.1021/cc050087q CCC: $33.50
Published on Web 01/06/2006

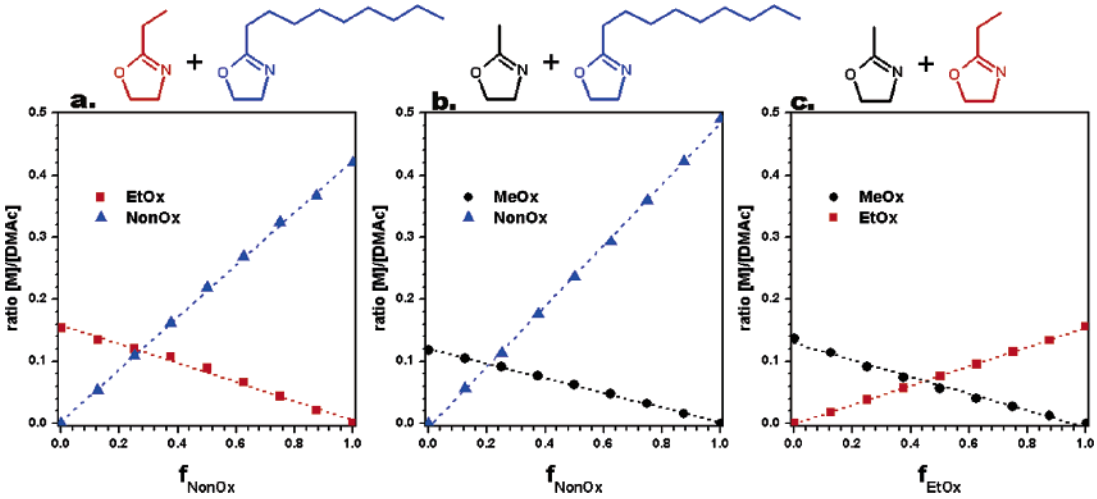

Figure 1. Ratios of monomer to solvent ([M]/[DMAc]) obtained by GC for $t = 0$ samples of the different copolymerizations plotted against fraction of the second monomer (f): a. EtOx:NonOx, b. MeOx:NonOx, and c. MeOx:EtOx. These graphs clearly demonstrate the gradual change in monomer composition within the investigated library.

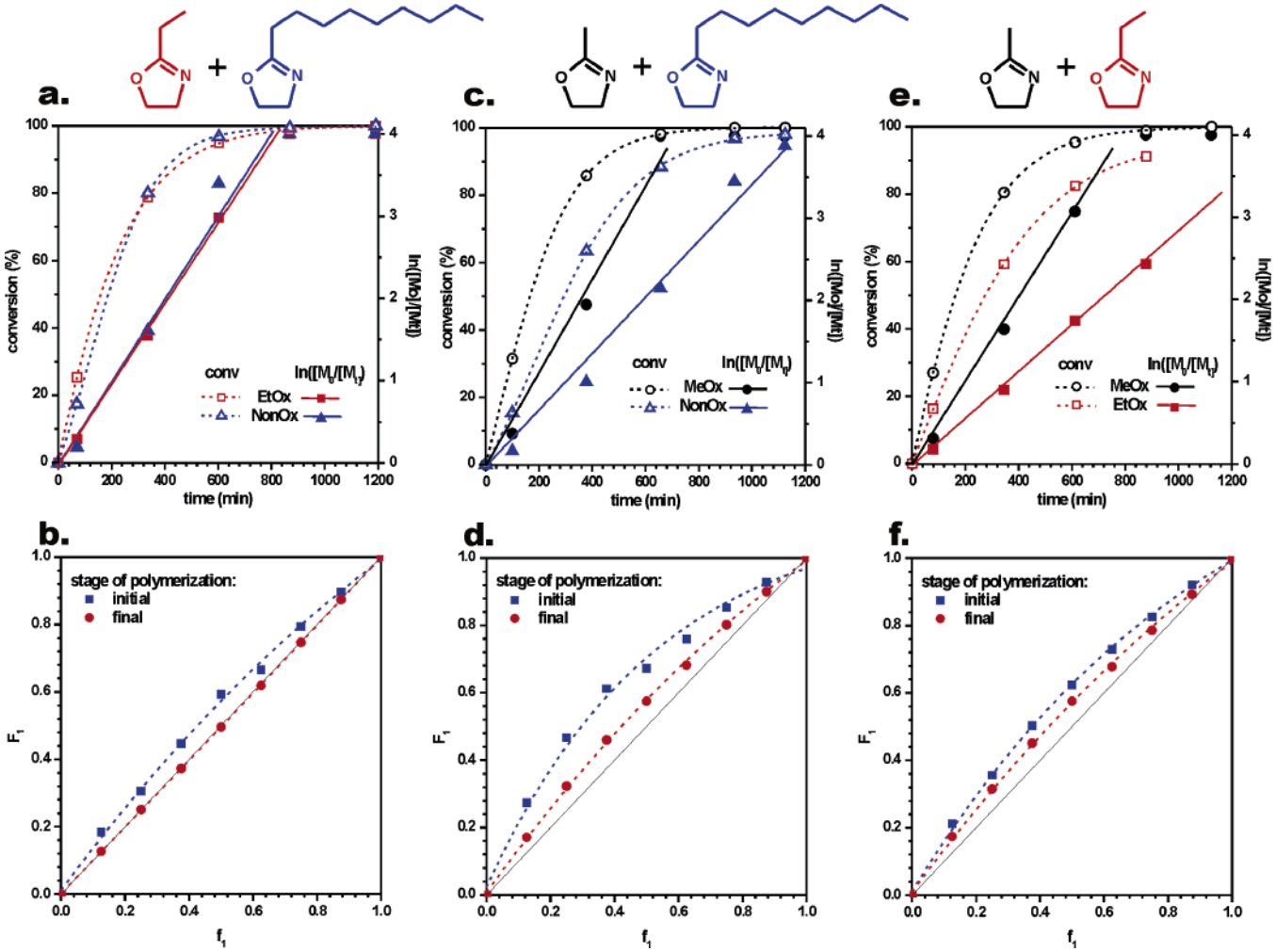

Figure 2. Top row: conversion ($\ln([M]_0/[M]_t)$ against time plots for 50 mol % copolymerizations (a, c, and e). Bottom row: relationship between the monomer feed (f_1) and the actual monomer incorporation (F_1) at the initial (~20% conversion) and final (>50% conversion) polymerization stages (b, d, and f). Both conversion and monomer incorporation are shown for EtOx:NonOx (a and b), MeOx:NonOx (c and d), and MeOx:EtOx (e and f) copolymerizations.

reactivity ratios at higher monomer conversion, the extended Kelen−Tüdös (KT) method can be applied.[19] The resulting reactivity ratios from both the MLTM and KT methods are summarized in Table 1. As expected, the reactivity ratios obtained for low conversion (initial r_1 and r_2) are similar for both calculation methods; however, the reactivity ratios for high conversion (final r_1 and r_2) from the different calculation methods differ significantly for the MeOx:NonOx and MeOx:EtOx copolymerizations. The KT method revealed similar reactivity ratios at low and high conversion for the

Table 1. Reactivity Ratios Determined for the 2-Oxazoline Copolymerizations Utilizing Both the Mayo−Lewis Terminal Model (MLTM) and Extended Kelen−Tüdös (KT) Method

M_1:M_2	method	initial r_1	initial r_2	final r_1	final r_2
EtOx:NonOx	MLTM	1.2 ± 0.2	0.7 ± 0.1	0.97 ± 0.01	0.99 ± 0.01
EtOx:NonOx	KT	1.23 ± 0.13	0.60 ± 0.05	0.91 ± 0.05	0.94 ± 0.03
MeOx:NonOx	MLTM	1.8 ± 0.3	0.3 ± 0.1	1.26 ± 0.05	0.66 ± 0.03
MeOx:NonOx	KT	1.94 ± 0.15	0.25 ± 0.04	1.83 ± 0.04	0.46 ± 0.02
MeOx:EtOx	MLTM	1.52 ± 0.1	0.54 ± 0.03	1.18 ± 0.04	0.65 ± 0.02
MeOx:EtOx	KT	1.67 ± 0.04	0.51 ± 0.04	1.63 ± 0.05	0.52 ± 0.04

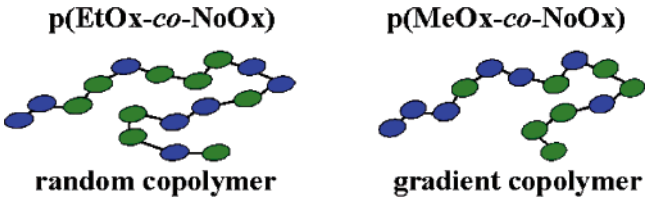

Figure 3. Schematic representation of the random and gradient monomer distributions throughout the EtOx:NonOx and MeOx:NonOx copolymers, respectively.

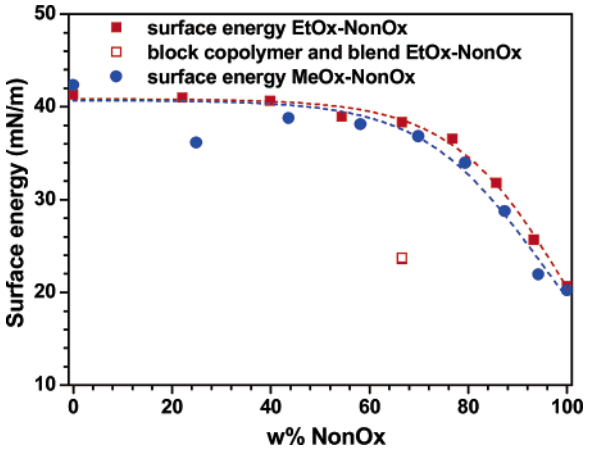

Figure 4. Surface energies calculated from the contact angles of diiodomethane and ethylene glycol for the copolymer series of MeOx:NonOx and EtOx:NonOx.

MeOx:EtOx copolymerizations, whereas the MeOx:NonOx and EtOx:NonOx copolymerizations revealed a more pronounced difference in reactivity ratios (utilizing the KT method) at the initial stage of the polymerizations, demonstrating a higher reactivity of the MeOx and EtOx, as compared to the NonOx during the initiation process. Furthermore, the reactivity ratios (KT method) revealed the formation of random copolymers for the EtOx:NonOx copolymerization (both final r_1 and $r_2 \approx 1$).[20] Finally, the copolymerizations of MeOx:NonOx and MeOx:EtOx resulted in the formation of gradient copolymers,[21] whereby the gradient is slightly more pronounced for the MeOx:NonOx copolymers.

The resulting library of copolymers was utilized to investigate the differences between random and gradient copolymers regarding surface and thermal properties. More specifically, the series containing MeOx:NonOx and EtOx:NonOx were compared, because they have a gradient or random composition, respectively (Figure 3), and pMeOx and pEtOx homopolymers have very similar surface and thermal properties. As a result, any differences observed between those series might be assigned to their different compositions. Other gradient copolymers were already shown to exhibit interesting mechanical and thermal properties.[22−24]

The synthesized copolymers were screened with regard to their surface energy in a high-throughput manner as described recently for a library of block copolyoxazolines.[25] Contact angles of spin-casted films were measured with two different test liquids (ethylene glycol and diiodomethane; four measurements per test liquid). The surface energy (SE) of the polymer films could be calculated from the difference between the contact angles of the polar and the apolar test liquids (the calculated SEs were generally obtained with <5% standard deviation). Figure 4 depicts the resulting SEs for the NonOx-containing copolymers against the wt % of NonOx present in the copolymers. The SEs are plotted against wt % NonOx, because wt % closer resembles the volume fraction NonOx and, thus, the theoretical surface coverage in the absence of preferential orientation. Both copolymer series show similar trends, whereby the SE changes from ∼42 mN·m^{-1} for the pMeOx and pEtOx to ∼21 mN·m^{-1} for the pNonOx. The similar trends for both series can be explained by the fact that the contact angle measurements are performed on a macroscopic scale (droplet size), whereas the small difference in composition for the copolymer series is a microscopic effect that is averaged out on this macroscopic level. Surprisingly, the SE does not decrease gradually with increasing NonOx content, but the presence of NonOx only becomes visible at approximately 50 wt % of NonOx. With lower NonOx contents, the SE is the same as for the pMeOx or pEtOx. The reason behind this peculiar behavior of the SEs of the copolymers is not understood at the moment. Moreover, the copolymers have a significantly higher SE when compared to a block copolymer or a blend of homopolymers of EtOx:NonOx (both 50 mol %; open square in Figure 4). This difference can be explained by the fact that the nonyl side-chains cannot orient to the surface without exposing the second monomer (MeOx or EtOx) to the surface in the copolymers, resulting in intermediate SE's; whereas, the NonOx segment can orient to the surface in the block copolymer or in the blend, resulting in a low surface energy close to the SE of pNonOx.

The influence of gradient or random monomer distribution on the thermal properties was investigated by DSC (Figure 5). Figure 5 shows the change of glass transition temperature (T_g), melting temperature (T_m), and the heat of fusion with incorporation of NonOx. Upon incorporation of NonOx into pMeOx or pEtOx, the T_g is decreasing due to the higher flexibility of the nonyl side-chains. At ∼90 wt % of NonOx, the glass transition disappears, which corresponds to the absence of a T_g for pNonOx in the DSC traces. In addition, the melting point of pNonOx decreases upon the incorpora-

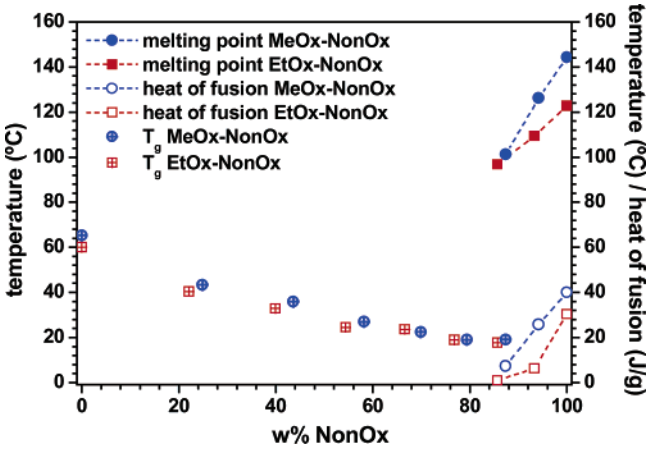

Figure 5. Thermal properties, T_g, T_m, and heat of fusion, of the copolymers consisting of MeOx:NonOx and EtOx:NonOx.

tion of MeOx or EtOx, since the crystallinity of the pNonOx is disturbed. The difference in T_m between the two series could be ascribed to small differences in polymer length, since different T_m's were obtained for both pNonOx homopolymers, as well. Corresponding to the decrease in T_m, the heat of fusion decreased upon the incorporation of MeOx or EtOx into pNonOx. Since the differences in T_m and heat of fusion most likely result from chain length differences, no conclusions on the effect of MeOx or EtOx incorporation on the crystallinity can be drawn except that the presence of a second monomer disturbs the crystallinity of the pNonOx side chains.

Conclusions. In conclusion, we have demonstrated the successful application of a high-throughput workflow for the investigation of random copolymerizations of 2-oxazolines regarding copolymerization parameters, surface properties, and thermal properties. Different reactivity ratios were determined for the initial and final polymer stages, revealing the formation of random (EtOx:NonOx) or gradient (MeOx:NonOx and MeOx:EtOx) copolymers. Contact angle measurements for the synthesized MeOx:NonOx and MeOx:EtOx copolymers revealed similar trends for both random and gradient copolymers; however, these copolymers showed significantly different surface energies, as compared to a block copolymer or a polymer blend. Moreover, the glass transition, melting temperatures, and heat of fusion changed in a similar manner within both MeOx:NonOx and MeOx:EtOx copolymer series. The small observed differences in T_m and heat of fusion most likely resulted from differences in polymer chain length and not from the difference between random or gradient monomer distributions.

In addition, it was demonstrated that the application of a high-throughput workflow to the synthesis and screening of a library of copolymers can result in both fundamental and application-directed knowledge at the same time.

Acknowledgment. The authors thank the Dutch Scientific Organization (NWO), the Dutch Polymer Institute (DPI), and the Fonds der Chemischen Industrie for financial support and Chemspeed Technologies for the collaboration.

Supporting Information Available. Experimental details are available as Supporting Information. This material is available free of charge via the Internet at http://pubs.acs.org.

References and Notes

(1) Tomalia, D. A.; Sheetz, D. P. *J. Polym. Sci., Part A: Polym. Chem.* **1966**, *4*, 2253−2265.
(2) Seeliger, W.; Aufderhaar, E.; Diepers, W.; Feinauer, R.; Nehring, R.; Thier, W.; Hellmann, H. *Angew. Chem.* **1966**, *20*, 913−927.
(3) Kagiya, T.; Narisawa, S.; Maeda, T.; Fukui, K. *Polym. Lett.* **1966**, *4*, 441−445.
(4) Aoi, K.; Okada, M. *Prog. Polym. Sci.* **1996**, *21*, 151−208.
(5) Kobayashi, S.; Uyama, H. *J. Polym. Sci., Part A: Polym. Chem.* **2002**, *40*, 192−209.
(6) Christova, D.; Velichkova, R.; Loos, W.; Goethals, E. J.; Du Prez, F. E. *Polymer* **2003**, *44*, 2255−2261.
(7) Levy, A.; Litt, M. *J. Polym. Sci., Part A1* **1968**, *6*, 1883−1894.
(8) Cai, G.; Litt, M. H. *J. Polym. Sci., Part A: Polym. Chem.* **1993**, *30*, 649−657.
(9) Guinot, P.; Bryant, L.; Chow, T. Y.; Saegusa, T. *Macromol. Chem. Phys.* **1996**, *197*, 1−17.
(10) Kagiya, T.; Matsuda, T.; Nakato, M.; Hirata, R. *J. Macromol. Sci., Chem.* **1972**, *A6*, 1631−1652.
(11) Hoogenboom, R.; Fijten, M. W. M.; Schubert, U. S. *J. Polym. Sci., Part A: Polym. Chem.* **2004**, *42*, 1830−1840.
(12) For a detailed description of the synthesis robot, see: Hoogenboom, R.; Schubert, U. S. *J. Polym. Sci., Part A: Polym. Chem.* **2003**, *41*, 2425−2434.
(13) The monomer conversion was calculated from the ratio of monomer to solvent (DMAc), whereby the solvent was applied as internal standard.
(14) The reactivity ratios are the ratios between the polymerization rate of monomer A with monomer A (k_{AA}) and the polymerization rate of monomer A with monomer B (k_{AB}).
(15) Madruga, E. L. *Prog. Polym. Sci.* **2002**, *27*, 1879−1924.
(16) Ziegler, M. J.; Matyjaszewksi, K. *Macromolecules* **2001**, *34*, 415−424.
(17) Saegusa, T.; Kobayashi, S.; Yamada, A. *Makromol. Chem.* **1976**, *177*, 2271−2283.
(18) Mayo, F. R.; Lewis, F. M. *J. Am. Chem. Soc.* **1944**, *66*, 1594−1601.
(19) Kelen, T.; Tüdös, F.; Turcsanyi, B.; Kennedy, J. P. *J. Polym. Sci., Polym. Chem.* **1977**, *15*, 3047−3074.
(20) If $r_1 \approx r_2 \approx 1$, the reactivity of monomers A and B to itself and to the other monomer are equal, resulting in a statistical distribution of the monomers throughout the polymer chains.
(21) If $r_1 > 1$ and $r_2 < 1$, the reactivity of monomer A to itself is larger than to monomer B, and the reactivity of monomer B to itself is lower than to monomer A.; therefore, monomer A will be incorporated faster in the beginning of the polymerization, and during the polymerization more and more of monomer B will be incorporated due to its increasing concentration, as compared to the concentration of monomer A. As a result, the polymer chains will have a gradient in the monomer composition.
(22) Kryszewski, K. *Polym. Adv. Technol.* **1998**, *9*, 244−259.
(23) Matyjaszewski, K.; Xia, J. *Chem. Rev.* **2001**, *101*, 2921−2990.
(24) Gray, M. K.; Zhou, H.; Nguyen, S. T.; Torkelson, J. M. *Macromolecules* **2004**, *37*, 5586−5595.
(25) Wijnans, S.; De Gans, B.-J.; Wiesbrock, F.; Hoogenboom, R.; Schubert, U. S.; *Macromol. Rapid Commun.* **2004**, *25*, 1958−1962.

CC050087Q

Supplementary information for:

The difference between random and gradient copoly(2-oxazoline)s

Richard Hoogenboom, Martin W. M. Fijten, Sanne Wijnans, Antje M. J. van den Berg, Hanneke M. L. Thijs and Ulrich S. Schubert*

Experimental Part

Materials

Solvents (except *N*,*N*-dimethylacetamide) were purchased from Biosolve Ltd and were used without further purification. *N*,*N*-Dimethylacetamide was obtained from Aldrich and dried over molecular sieves (size 4 Å). 2-Methyl-2-oxazoline (Aldrich), 2-ethyl-2-oxazoline (Aldrich), benzyl bromide (Acros Organics) and 2-nonyl-2-oxazoline (kindly provided by Henkel) were distilled over barium oxide and stored under argon.

Instruments

Reactions were carried out on a Chemspeed ASW2000 automated synthesizer equipped with 2 reactor blocks containing 16 reaction vessels of 13 mL. The reactors could be heated by a Huber Unistat Tango (heating range: -40 ºC to 145 ºC) *via* their double jackets. All reactor vessels were equipped with cold-finger reflux condensers that could be cooled or heated from –5 °C to 50 °C. An inert atmosphere was maintained by applying a 1.1 bar argon flow over the reactors and a 1.5 bar argon flow through the hood of the automated synthesizer.

GC measurements were performed on an Interscience Trace GC with a RTX-5 Trace Column and a PAL autosampler. For the injection of polymerization mixtures, a special Interscience liner with additional glass wool was used. Gel permeation chromatography (GPC) was measured on a Shimadzu system equipped with a SCK-10A system controller, a LC-10AD pump, a RID-10A refractive index detector and a PL gel 5 µm Mixed-D column at 50 ºC utilizing a chloroform/triethylamine/isopropanol (94/4/2) mixture as eluent at a flow rate of 1 mL·min^{-1} or a Waters system with a 1515 pump, a 2414 refractive index detector and a Waters Styragel HT4 column utilizing N,N-dimethylformamide with

$5 \cdot 10^{-3}$ M NH_4PF_6 as eluent at a flow rate of 0.5 mL·min^{-1} at 50 °C. The molecular weights were calculated on the basis of poly(styrene) standards.

Thermal transitions were determined on a DSC 204 F1 Phoenix by Netzsch under a nitrogen atmosphere with heating and cooling rates of 40 K·min^{-1} (three measurements per sample after an initial first heating run that was not considered for the subsequent calculations); melting points were measured with a heating rate of 10 K·min^{-1}and a cooling rate of 40 K·min^{-1}. Contact angle measurements were performed on polymer films that were prepared by spincoating of chloroform solutions (20 mg/mL) of the polymers on pre-cleaned microscopy slides at 1000 rpm during 90 seconds using a WS-400/500 series spin coater from Laurell Technologies Corporation. An OCA30 optical contact angle measuring instrument from Dataphysics was used to determine the contact angles of both diiodomethane and ethyleneglycol as apolar and polar testliquids, respectively.

Parallel polymerizations

To obtain an inert atmosphere, the hood of the ASW2000 synthesis robot was flushed for at least 90 minutes with argon before starting the polymerization procedure. An inert atmosphere was created inside the individually heatable reaction vessels by performing three cycles of heating (120 ºC) under vacuum (15 min at ~ 25 mbar) followed by argon flushing (1 min). During the polymerizations, the temperature of the cold-finger reflux condensers was set to – 5 ºC. Stock solutions of the 2-oxazoline monomers and benzyl bromide in *N*,*N*-dimethylacetamide and were transferred into the 13 mL reaction vessels at different ratios resulting in 3.2 mL polymerization mixtures with 1.25 M total monomer concentration and a monomer to initiator ratio of 60. After sampling 100 µL aliquots to 2 mL vials prefilled with 1.0 mL of chloroform saturated with water, the mixtures were heated to 100 ºC and vortexed at 600 rpm for 20 hours. During the 20 hours polymerization time, samples (100 µL aliquots) were taken in time to 2 mL vials prefilled with 1.0 mL chloroform saturated with water. Subsequently, water was added into the reaction vessels to terminate the reactions and the mixtures were collected in sample vials.